

Geoelectrical Method to Determine Andesite Rock Potential in Kepuh, Ciwandan District, Cilegon City

Deno Ambar Arum^{a,*}, Nana Sulaksana^a, Euis Tintin Yuningsih^a

^a Faculty of Geological Engineering, University of Padjadjaran, Dipatiukur Street, Bandung City, 40132, Indonesia

Corresponding author: *deno18001@mail.unpad.ac.id

Abstract—The Kepuh area has abundant andesite rock resources. These rocks can be used as building materials and for other infrastructure. Based on this, it is necessary to research the potential of andesite resources. The tools used for this research are a resistivity meter, meter, current and potential wires, electrodes, hammer, battery, a global positioning system (GPS), handy talky, laptop and software (IP2win). The research applies the geoelectric method, which measures rock resistivity values. This geoelectric investigation uses the Schlumberger array. The advantages of the Schlumberger array are that fewer electrodes need to be moved for each sounding, and the cable length for the potential electrodes is shorter. Schlumberger soundings generally have better resolution, greater probing depth, and less time-consuming field deployment. The data obtained from the measurements were processed using IP2win software by entering the magnitude of the current, the value of the potential difference, and the electrode. The results of geoelectrical interpretation, the rocks found in the research area are topsoil, tuff, and andesite lava. The resistivity value of the topsoil in the study area mostly varies from 26.3 – 116 ohms – meters, tuff has resistivity values range of 18.8 – 84.2 ohms – meters, and Andesite lava has a resistivity range of 128 - 570 ohms – meters. The average thickness of topsoil is 1.4 meters, the average thickness of tuff is 25.9 meters, and the average thickness of andesite lava is 42.6 meters. Based on the average thickness, andesite rock can be the main commodity.

Keywords—Andesite; geoelectric; resistivity; Schlumberger array.

Manuscript received 6 Aug. 2021; revised 25 Sep. 2021; accepted 13 Dec. 2021. Date of publication 31 Oct. 2022.
IJASEIT is licensed under a Creative Commons Attribution-Share Alike 4.0 International License.



I. INTRODUCTION

Volcanic rocks, including igneous rocks, have favorable aggregate properties. Therefore, they are frequently applied in various construction industry segments [1]. Andesite is one of the igneous rocks. It is often used as a mineral additive in concrete, asphalt [2]–[4], building stones [5], and so on. Andesite is the most complex of all magmatic rocks and much more complex than basalt and granite. The Andesite is different from both the crust and mantle source, and it can also be formed by basal fractional crystallization or by magmatic mixing [6].

The Ciwandan District area has abundant andesite rock resources, so it can be utilized. Based on this, it is necessary to research to determine the distribution and thickness of andesite rocks. The research uses geophysical methods. Nowadays, geophysical methods are increasingly used because they are cheaper and faster than other conventional geological methods [7]–[9]. Applied geophysics bases its success on the ability to estimate subsoil properties in a non-invasive manner. Rock properties are reconstructed through

indirect measurements carried out on the Earth's surface. In such a way, activities such as drilling in the subsoil can be avoided [10], which could alter or damage the target being investigated and are, in any case, extremely expensive. Furthermore, the information derived from borehole drilling always presents a local character, whereas geophysical imaging furnishes a regional reconstruction of buried structures' main features, at the scale of interest, in a faster and more economical fashion [11]. This method is widely used to address a variety of near-surface exploration problems including hydrogeological (e.g., [12]; [13]; [14]) environmental, and geotechnical studies (e.g., [15]; [16]; [17]). In addition, the results of 1D inversion of electrical sounding may be used in constituting starting models or a priori information for 2D/3D interpretations [18].

II. MATERIALS AND METHOD

The tools used in this research are a resistivity meter, meter, current and potential wires, electrodes, hammer, battery, GPS (Global Positioning System) and handy talky, laptop, and IP2win software. The research area is located in Kepuh

Village, Ciwandan District, Cilegon City. This study was carried out in two stages. The first is to study secondary data, including geological maps, topographic maps, and reports from previous investigations, as a reference for interpreting and analyzing the geological conditions of the study area. The second method is the geoelectric method, which measures rock resistivity values. Before carrying out the geoelectric method, it is necessary to determine the geoelectric location point by adjusting the secondary data collected to obtain the geoelectric measurement point. The location point consists of 12 points (Fig. 1).

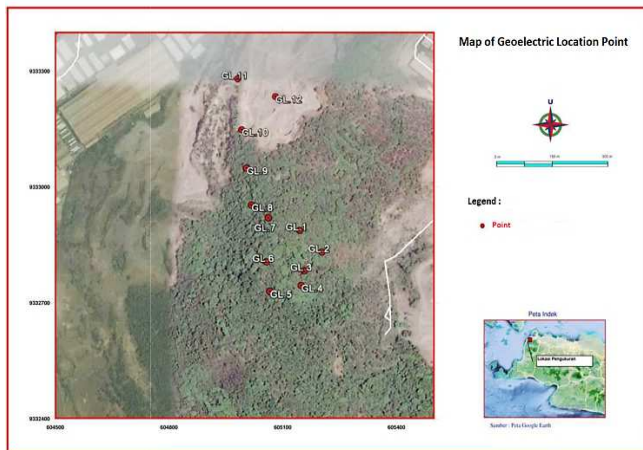


Fig. 1 Geoelectric recording point

This geoelectric investigation uses the arrangement of the Schlumberger array (Fig. 2). The Schlumberger configuration is an excellent geoelectrical method for vertical electrical sounding (VES). Vertical Electrical Sounding (VES) estimates the depth-wise layer resistivities and thicknesses. The electrical resistivity measurement requires a four-electrode arrangement, two for injecting current into the ground, and the other for measuring the resulting potential. Schlumberger configuration is most commonly used for VES data collection [19]. VES method was designed to provide vertical 1-D profiles of resistivity [20] [21] [22].

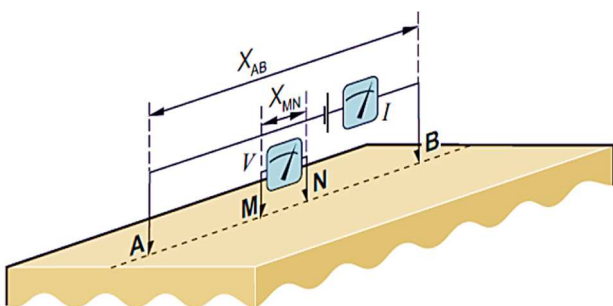


Fig. 2 Schlumberger Configuration Array [23]

The data obtained from the measurement of the Schlumberger configuration will be processed with the IP2win software by entering the magnitude of the current, the value of the potential difference, and the electrode spacing into the IP2win software to calculate the geometry factor and then calculate the rock resistivity value. The resistivity obtained is the apparent resistivity because rocks below the earth's surface consist of many layers with different resistivity

values, so the actual resistivity is not obtained. The way to find out the real resistivity is by the inversion process until the smallest error is obtained (usually less than 10%).

III. RESULTS AND DISCUSSION

Each rock layer has resistivity characteristics, as shown in Table 1 [24]

TABLE I
RESISTIVITY VALUES OF SOME EARTH MATERIALS

Material	Resistivity (Ωm)
Granite	200-100000
Andesite	$1.7 \times 10^2 - 45 \times 10^4$
Basalt	200-100000
Limestone	500-10000
Sandstone	200-8000
Shales	20-2000
Sand	1-1000
Clay	1-100
Dry Gravel	600-10000
Alluvium	10-800
Gravel	100-600

The data processing results with IP2win software are in the form of 2-dimensional curves and tables. The graph consists of curves in black, blue, and red. The blue curve represents the thickness and boundary of the layer at the sounding point, the red curve is the standard curve or reference curve, and the black curve is the research data curve. The data processing results can be seen in Fig. 3 to Fig. 14.

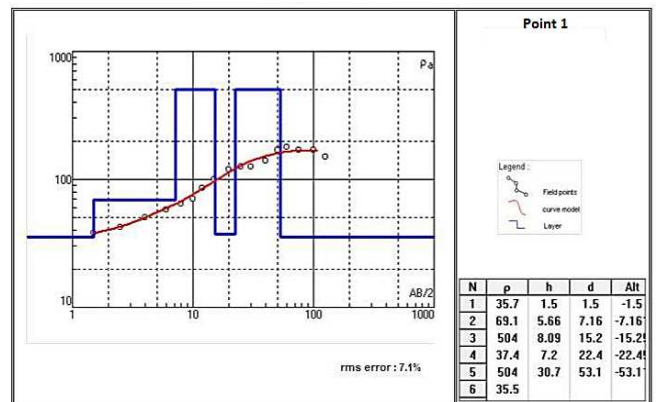


Fig. 3 Geoelectric Point 1

The results of interpretation from Fig. 3 are in Table 2. Table 2 shows that Andesite has resistivity 504 Ωm .

TABLE II
INTERPRETATION OF FIGURE 3

Depth (m)	Resistivity (Omh-m)	Lithology	Thickness (m)
0.00 - 1.5	35.7	Top Soil	1.5
1.5 - 7.16	69.1	Tuff	5.66
7.16 - 15.2	504	Andesite lava	8.09
15.2 - 22.4	37.4	Tuff	7.2
22.4 - 53.1	504	Andesite Lava	30.7
> 53.1	35.5	Tuf	?

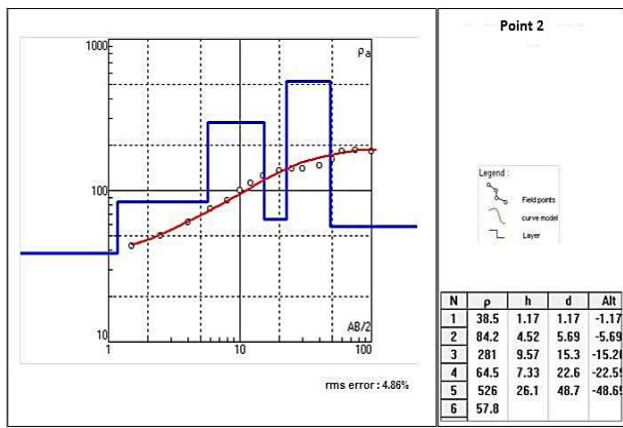


Fig. 4 Geoelectric Point 2

The results of interpretation from Fig. 4 are in Table 3. Table 3 shows that Andesite has resistivity values range of 281-526 Ωm .

TABLE III
INTERPRETATION OF FIGURE 4

Depth (m)	Resistivity (Omh-m)	Lithology	Thickness (m)
0.00 - 1.17	38.5	Top Soil	1.17
1.17 - 5.69	84.2	Tuff	4.52
5.69 - 15.3	281	Andesite Lava	9.57
15.3 - 22.6	64.5	Tuff	7.33
22.6 - 48.7	526	Andesite Lava	26.1
> 48.7	57.8	Tuff	?

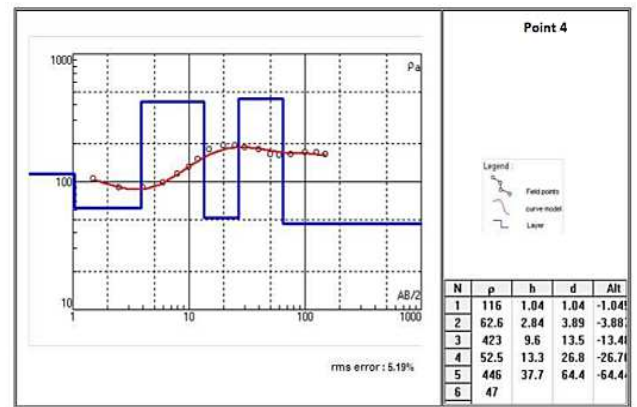


Fig. 6 Geoelectric Point 4

The results of interpretation from Fig. 6 are in Table 5. Table 5 shows that Andesite has resistivity values range of 423-446 Ωm .

TABLE V
INTERPRETATION OF FIGURE 6

Depth (m)	Resistivity (Omh-m)	Lithology	Thickness (m)
0.00 - 1.04	116	Top Soil	1.04
1.04 - 3.89	62.6	Tuff	2.84
3.89 - 13.5	423	Andesite Lava	9.6
13.5 - 26.8	52.5	Tuff	13.3
26.8 - 64.4	446	Andesite Lava	37.7
> 64.4	47	Tuff	?

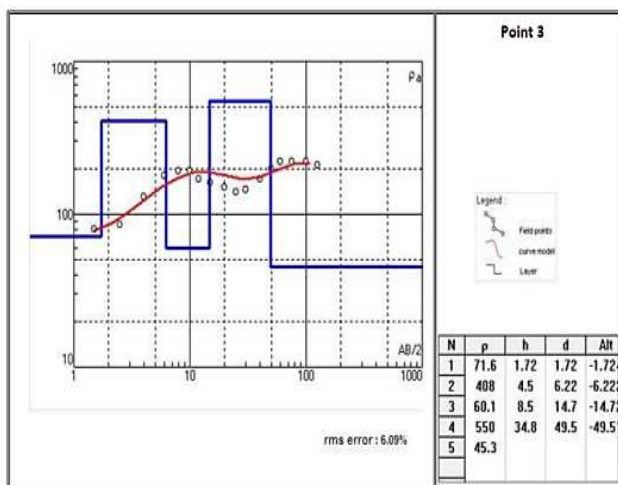


Fig. 5 Geoelectric Point 3

The results of interpretation from Fig. 5 are in Table 4. Table 4 shows that Andesite has resistivity values range of 408-550 Ωm .

TABLE IV
INTERPRETATION OF FIGURE 5

Depth (m)	Resistivity (Omh-m)	Lithology	Thickness (m)
0.00 - 1.72	71.6	Top Soil	1.72
1.72 - 6.22	408	Andesite Lava	4.5
6.22 - 14.7	60.1	Tuff	8.5
14.7 - 49.5	550	Andesite Lava	34.8
>49.5	45.3	Tuff	?

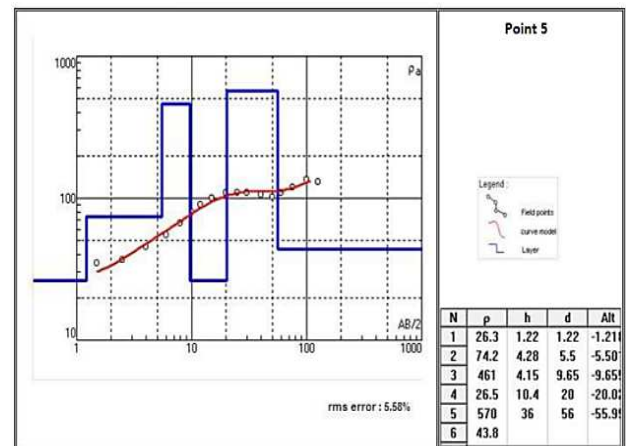


Fig. 7 Geoelectric Point 5

The results of interpretation from Fig. 7 are in Table 6. Table 6 shows that Andesite has resistivity values range of 461-570 Ωm .

TABLE VI
INTERPRETATION OF FIGURE 7

Depth (m)	Resistivity (Omh-m)	Lithology	Thickness (m)
0.00 - 1.22	26.3	Top Soil	1.22
1.22 - 5.5	74.2	Tuff	4.28
5.5 - 9.65	461	Andesite Lava	4.15
9.65 - 20	26.5	Tuff	10.4
20 - 56	570	Andesite Lava	36
> 56	43.8	Tuff	?

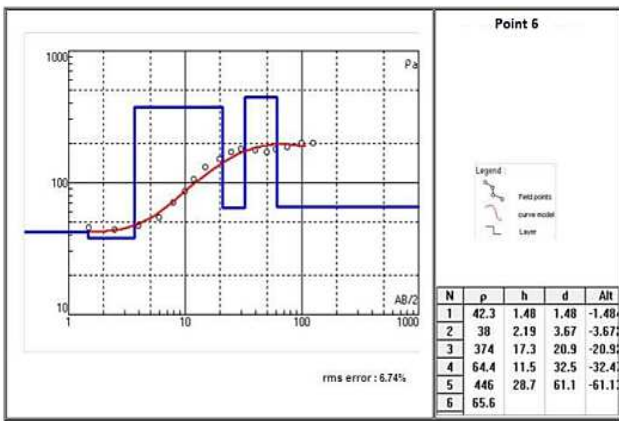


Fig. 8 Geoelectric Point 6

The results of interpretation from Fig. 8 are in Table 7. Table 7 shows that Andesite has resistivity values range of 374-446 Ω m.

TABLE VII
INTERPRETATION OF FIGURE 8

Depth (m)	Resistivity (Omh-m)	Lithology	Thickness (m)
0.00 - 1.48	42.3	Top Soil	1.04
1.48 - 3.67	38	Tuff	2.84
3.67- 20.9	374	Andesite Lava	9.6
20.9- 32.5	64.4	Tuff	13.3
32.5- 61.1	446	Andesite Lava	37.7
> 61.1	65.6	Tuff	?

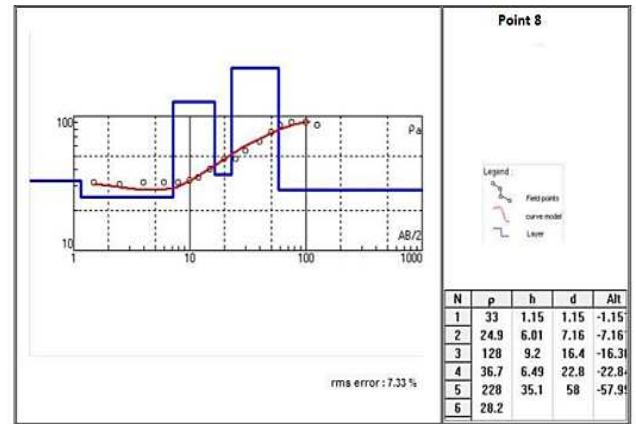


Fig.10 Geoelectric Point 8

The results of interpretation from Fig. 10 are in Table 9. Table 9 shows that Andesite has resistivity values range of 128-228 Ω m.

TABLE IX
INTERPRETATION OF FIGURE 10

Depth (m)	Resistivity (Omh-m)	Lithology	Thickness (m)
0.00 - 1.15	33	Top Soil	1.15
1.15 - 7.16	24.9	Tuff	6.01
7.16- 16.4	128	Andesite Lava	9.2
16.4- 22.8	36.7	Tuff	6.49
22.8- 58	228	Andesite Lava	35.1
> 58	28.2	Tuff	?

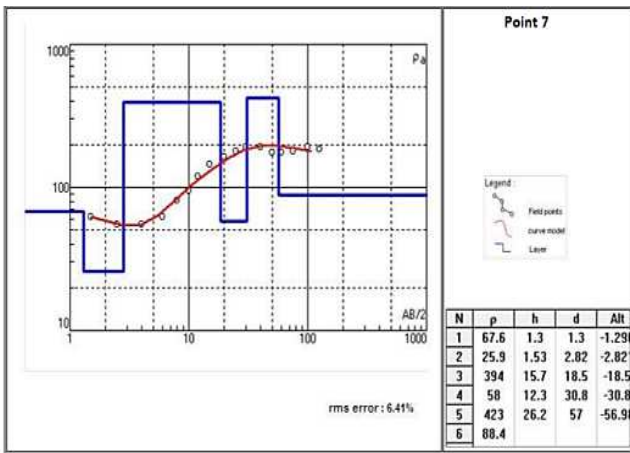


Fig. 9 Geoelectric Point 7

The results of interpretation from Fig. 9 are in Table 8. Table 8 shows that Andesite has a resistivity value range of 394-423 Ω m.

TABLE VIII
INTERPRETATION OF FIGURE 9

Depth (m)	Resistivity (Omh-m)	Lithology	Thickness (m)
0.00 - 1.3	67.6	Top Soil	1.3
1.3 - 2.82	25.9	Tuff	1.53
2.82- 18.5	394	Andesite Lava	15.7
18.5- 30.8	58	Tuff	12.3
30.8- 57	423	Andesite Lava	26.2
> 57	88.4	Tuff	?

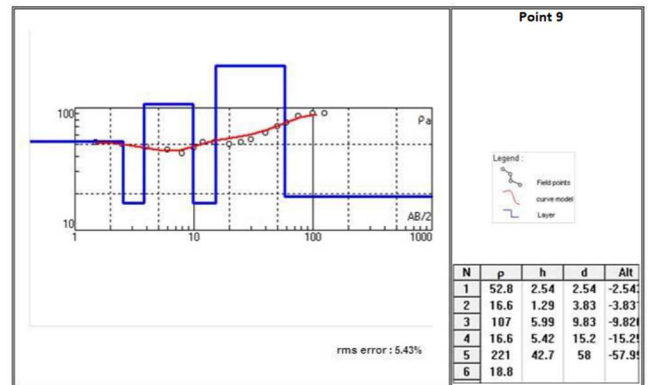


Fig. 11 Geoelectric Point 9

The results of interpretation from Fig. 11 are in Table 10. Table 10 shows that Andesite has resistivity values range of 107-221 Ω m.

TABLE X
INTERPRETATION OF FIGURE 11

Depth (m)	Resistivity (Omh-m)	Lithology	Thickness (m)
0.00 - 2.54	52.8	Top Soil	2.54
2.54 - 3.83	16.6	Tuff	1.29
3.83- 9.83	107	Andesite Lava	5.99
9.83- 15.2	16.6	Tuff	5.42
15.2- 58	221	Andesite Lava	42.7
> 58	18.8	Tuff	?

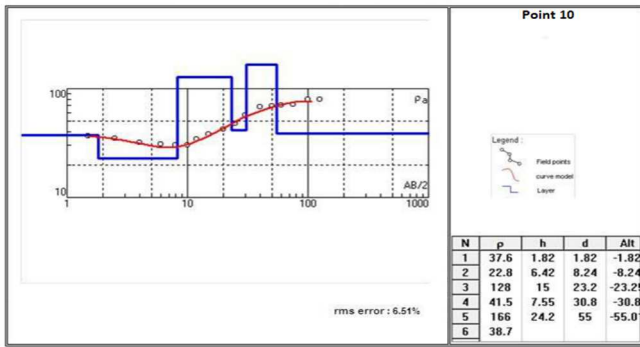


Fig. 12 Geoelectric Point 10

The results of interpretation from Fig. 12 are in Table 11. Table 11 shows that Andesite has resistivity values range of 128-116 Ω m

TABLE XI
INTERPRETATION OF FIGURE 12

Depth (m)	Resistivity (Omh-m)	Lithology	Thickness (m)
0.00 - 1.82	37.6	Top Soil	1.82
1.82 - 8.24	22.8	Tuff	6.42
8.24- 23.2	128	Andesite Lava	15
23.2- 30.8	41.5	Tuff	7.55
30.8- 55	166	Andesite Lava	24.2
> 55	38.7	Tuff	?

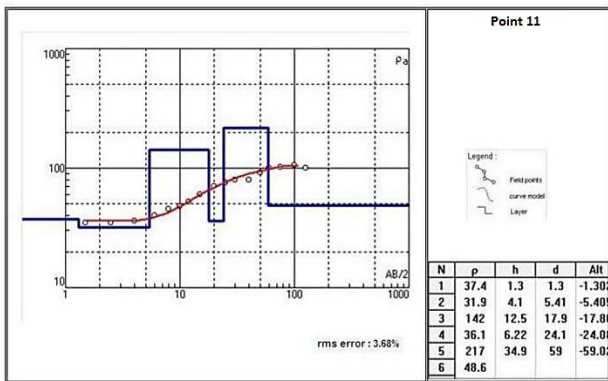


Fig. 13 Geoelectric Point 11

The results of interpretation from Fig. 13 are in Table 12. Table 12 shows that Andesite has resistivity values range of 142-217 Ω m.

TABLE XII
INTERPRETATION OF FIGURE 13

Depth (m)	Resistivity (Omh-m)	Lithology	Thickness (m)
0.00 - 1.3	37.4	Top Soil	1.04
1.3 - 5.41	31.9	Tuff	2.84
5.41- 17.9	142	Andesite Lava	9.6
17.9- 24.1	36.1	Tuff	13.3
24.1- 59	217	Andesite Lava	37.7
> 59	48.6	Tuff	?

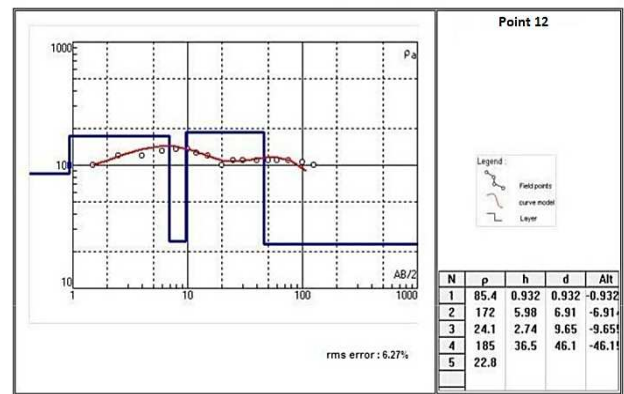


Fig. 14 Geoelectric Point 12

The results of interpretation from Fig. 14 are in Table 13. Table 13 shows that Andesite has resistivity values range of 172-185 Ω m.

TABLE XIII
INTERPRETATION OF FIGURE 14

Depth (m)	Resistivity (Omh-m)	Lithology	Thickness (m)
0.00 - 0.9	85.4	Top Soil	0.9
0.9 - 6.91	172	Andesite Lava	5.98
6.91- 9.65	24.1	Tuff	2.74
9.65- 46.1	185	Andesite Lava	36.5
>46.1	22.8	Tuff	?

TABLE XIV
INTERPRETATION OF ROCK THICKNESS FOR EACH GEOELECTRIC POINT

NO	Point	Top Soil	Tuff	Andesite Lava
1	1	1.5	29.7	38.8
2	2	1.17	33.1	35.7
3	3	1.72	29	39.3
4	4	1.04	21.7	47.3
5	5	1.22	28.7	40.5
6	6	1.48	22.6	46
7	7	1.3	26.8	41.9
8	8	1.15	24.5	44.3
9	9	2.54	18.7	48.7
10	10	1.82	29	39.2
11	11	1.3	21.3	47.4
12	12	0.9	26.6	42.4

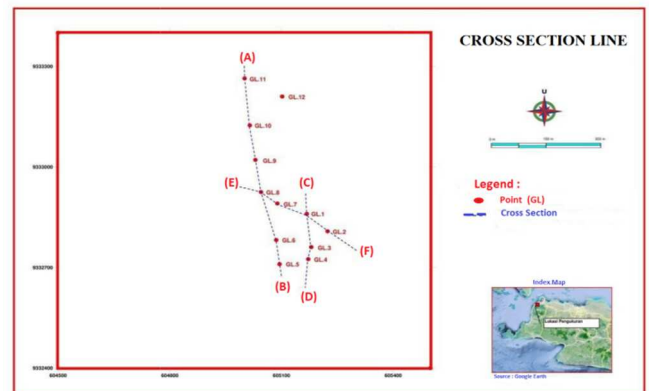


Fig. 15 Cross Section Line

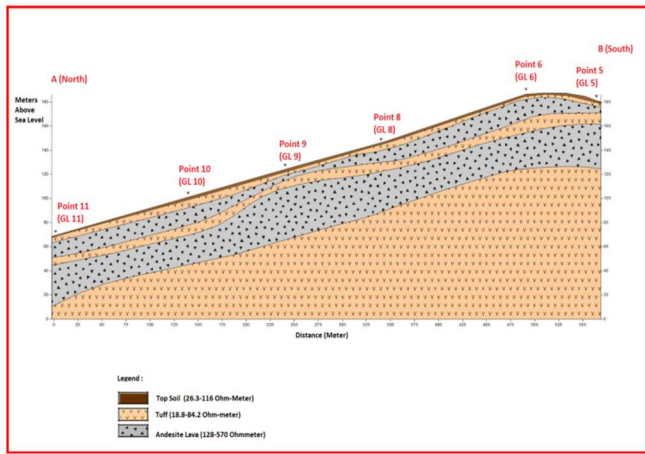


Fig. 16 A-B Cross Section

A-B cross section (Fig. 16) consists of 6 layers. The first layer is topsoil with a thickness between 1.15 – 2.54 meters, and the resistivity is between 26.3-52.8 Ωm . The second layer is tuff, with a thickness of 1.29 – 6.01 meters, and the resistivity is between 16.6-74.2 Ωm . The third layer is andesite lava with thickness between 5.99 – 17 meters, and the resistivity is between 107-461 Ωm . The fourth layer is tuff with a thickness between 5.42 – 11.55 meters and the resistivity are between 16.6-64 Ωm . The fifth is andesite lava with a thickness between 24.2 – 42.7 meters and a resistivity between 166-570 Ωm . The sixth layer is tuff, with resistivity between 18.8-65.6 Ωm .

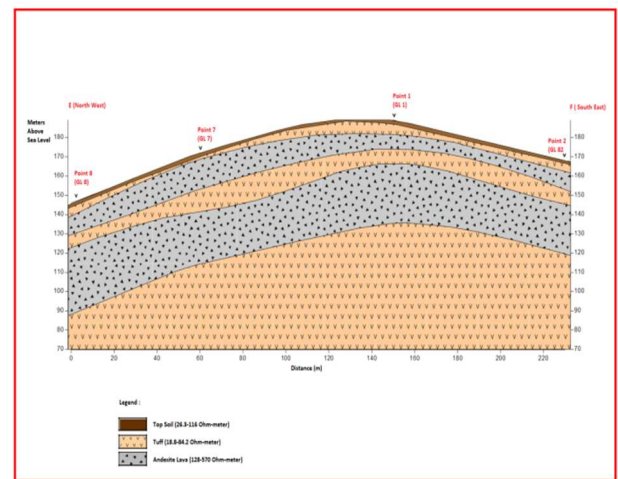


Fig. 18 E-F Cross Section

E-F cross section (Fig. 18) consists of 6 layers. The first layer is topsoil with a thickness between 1.17 – 1.48 meters, and the resistivity is between 35.7 – 67.6 Ωm . The second layer is tuff, with a thickness of 1.53 – 5.66 meters, and the resistivity is between 25.9 – 84.2 Ωm . The third layer is andesite lava with a thickness between 8.09 – 17.3 meters, and the resistivity is between 281-504 Ωm . The fourth layer is tuff, with a thickness between 7.2 – 12.3 meters, and the resistivity is between 37.4-64.5 Ωm . The fifth is andesite lava with a thickness between 26.1 – 30.7 meters and the resistivity between 423-526 Ωm . The sixth layer is tuff with a resistivity between 33.5-88.4 Ωm .

IV. CONCLUSION

The rocks found at the investigation site are topsoil, tuff, and andesite lava. Topsoil has resistivity values range 26.3 – 116 ohms – meters, tuff has resistivity values range of 18.8 – 84.2 ohms – meters, and the andesite lava has a resistivity range of 128 - 570 ohms – meters. The average thickness of topsoil is 1.4 meters, the average thickness of tuff is 25.9 meters, and the average thickness of andesite lava is 42.6 meters. Based on the average thickness, andesite rock can be the main commodity.

ACKNOWLEDGMENT

The authors thank my parent, siblings, friends, and lecturers for warm support, inspiration and thoughtful guidance.

REFERENCES

- [1] B. Czinder, B. Vasarhelyi, A. Torok, "Long-term abrasion of rocks assessed by micro-Deval tests and estimation of the abrasion process of rock types based on strength parameters". *Eng. Geol.* vol.282. Mar. 2021. <https://doi.org/10.1016/j.enggeo.2021.105996>.
- [2] M. Davraz, H. Ceylan, I. B. Topcu, T. Uygunoglu, "Pozzolanic effect of andesite waste powder on mechanical properties of high strength concrete". *Con and Build. Mat.* vol. 165, pp. 494-503. Mar. 2018. <https://doi.org/10.1016/j.conbuildmat.2018.01.043>.
- [3] Y. Miao, X. Liu, Y. Hou, J. Li, L. Wang, "Packing Characteristics of aggregate with consideration of particle size and morphology". *Appl. Sci.* vol. 9, no. 5, pp. 869. Feb. 2019. <https://doi.org/10.3390/app9050869>.
- [4] X. Zhou, G. Zhao, S. Tighe, M. Chen, S. Wu, S. Adhikari, Y. Gao, "Quantitative comparison of surface and interface adhesive properties of fine aggregate asphalt mixtures composed of basalt, steel slag, and

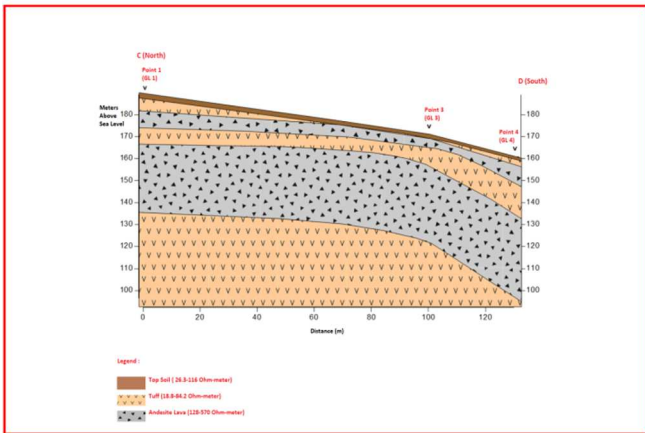


Fig. 17 C-D Cross Section

C-D cross section (Fig. 17) consists of 6 layers. The first layer is top soil with thickness between 1.04 – 1.72 meters and the resistivity is between 35.7-116 Ωm . The second layer is tuff with thickness of 2.84 – 5.6 meters and the resistivity is between 62.6-69.1 Ωm . The third layer is andesite lava with thickness between 4.5 – 9.6 meters and the resistivity is between 408-504 Ωm . The fourth layer is tuff with thickness between 7.2 – 13.3 meters and the resistivity is between 37.4-60.1 Ωm . The fifth is andesite lava with thickness between 30.7 – 37.7 meters and the resistivity is between 446-550 Ωm . The sixth layer is tuff with a resistivity between 35. 5-47 Ωm .

- andesite". *Con and Build, Mat.* vol. 246. Jun. 2020. <https://doi.org/10.1016/j.conbuildmat.2020.118507> .
- [5] S. E. Celik, J. Gulen, H. A. Viles, "Evaluating the effectiveness of DAP as a consolidant on Turkish building stones". *Con and Buil, Mat.* vol. 262. Nov. 2020. <https://doi.org/10.1016/j.conbuildmat.2020.120765> .
- [6] S. Jiao, Q. Zhang, Y. Zhou, W. Chen, X. Liu, G. Gopalakhrisan, "Progress and challenges of big data research on petrology and geochemistry". *Sol. Ear. Sci.* vol. 3, no. 4, pp. 105-114. Dec. 2018. <https://doi.org/10.1016/j.sesci.2018.06.002> .
- [7] A. Aliyanezhadi, S. R. Mehrnia, S. Kimiagar, H. Rahimi, N. Sadrmohammadi, "Evaluation of GPR method in identificaton hidden faults of Alluvial deposits in north Persian Gulf artificial lake, twenty-two ditrict of Tehran". *J. Of App. Geophy.* vol. 179. Aug. 2020. <https://doi.org/10.1016/j.jappgeo.2020.104108> .
- [8] F. H. Al-Menshed, J.M. Thabit, "Comparison between VES and 2d Imaging Techniques for Delinating Subsurface Plume of Hydrocarbon Contaminated Water Southeast of Karbala City, Iraq". *Arab. Jou of Geosci.* vol. 11, no. 7, pp. 1-9. Apr. 2018. <https://doi.org/10.1007/s12517-018-3479-5> .
- [9] S. M. Sharafeldin, K.S. Essa et al, "Shallow geophysical techniques to investigate the groundwater table at the Great Pyramids of Giza, Egypt ". *Geosci. Instrum. Method.* vol. 8, no. 1, pp. 29-43. Feb. 2019. <https://doi.org/10.5194/gi-8-29-2019> .
- [10] A. Susilo, Sunaryo, F. Fina, and Sarjiyana, "Fault Analysis In Pohgajih Village, Blitar, Indonesia Using Resistivity Method For Hazard Risk Reduction". *Int. Jour. of Geo.* vol.14, no. 41, pp.111-118, Jan. 2018 .
- [11] A. Troiano, and M. G. Giuseppe, "Application of principal component analysis to geoelectric recordings". *J. Of app. Geophy.* vol. 178. Apr. 2020. <https://doi.org/10.1016/j.jappgeo.2020.104038> .
- [12] R. Eissa, N. Cassidy, J. Pringle, I. Stimpson, "Electrical resistivity tomography array comparisons to detect cleared-wall foundations in brownfield sites". *Quar. Jour. Of Eng. Geo. Hyd.* vol. 53, no. 1, pp. 137-144. Jun. 2019. <https://doi.org/10.1144/qjegh2018-192> .
- [13] N. Skibbe, T. Ggunther, M. M. Petke, "Improved hydrogeophysical imaging by structural coupling of two-dimensional magnetic resonance and electrical resistivity tomography". *Geophy.* vol 86, no. 5. pp. 1-56. Jun. 2021. <https://doi.org/10.1190/geo2020-0593.1> .
- [14] A. Rastergania, G. Reza et al, "Assessment of the engineering geologiv]cal characteristics of the Bazoft dam site, SW Iran". *Quar. Jou of Eng. Geo and hydr.* vol . 52, no. 3, pp. 360-374. Feb. 2019. <https://doi.org/10.1144/qjegh2017-042> .
- [15] M. Kiernan, D. Jackson, J. Montgomery, J. B. Anderson, B. W. Mcdonald, K. C. Davis, "Characterization of a Karst Site using Electrical Resistivity Tomography and Seismic Full Waveform Inversion". *J. Of Env, and Eng. Geophy.* vol. 26, no. 1, pp. 1-11. Mar. 2021. <https://doi.org/10.32389/JEEG20-045> .
- [16] W. J. Koehn, E. Stacey. T. Kulesza, D. R. Steward, "Characterizing Riverbed Heterogeneity across Shifts in River Discharge through Temporal Changes in Electrical Resistivity". *J. Of Env, and Eng. Geophy.* vol. 25, no. 4. pp. 581-587. Dec. 2020. <https://doi.org/10.32389/JEEG20-049> .
- [17] M. A. Iravani, J. Deparis, H. Davarzani, S. Colombano. R. Guerin, A. Mainault, "Complex Electrical Resistivity and Dielectric Permittivity Responses to Dense Non-aqueous Phase Liquids' Imbibition and Drainage in Porous Media: A Laboratory Study". *J. Of Env, and Eng. Geophy.* vol. 25, no. 4. pp. 557-567. Dec. 2020. <https://doi.org/10.32389/JEEG20-050> .
- [18] R. Ghanati, and M. M. Petke, "A homotopy continuation inversion of geoelectrical sounding data". *J. Appl. Geophys.* Vo. 191. Aug. 2020. <https://doi.org/10.1016/j.jappgeo.2021.104356> .
- [19] N. C. Mondal, "Geoelectrical signatures for detecting water-bearing zones in a micro-watershed of granitic terrain from Southern India". *J. Appl. Geophys.* Vol. 191. Aug. 2021. <https://doi.org/10.1016/j.jappgeo.2021.104361> .
- [20] I. C. Alle, M. Desclotres, J. M. Vouillamoz, N. Yalo, F. M. Lawson, A. C. Adihou, "Why 1D electrical resistivity techniques can result in inaccurate siting of boreholes in hard rock aquifers and why electrical resistivity tomography must be preferred: The example of Benin, West Africa". *J. Afr. Earth Sci.* vol. 139, pp. 341-353. Mar. 2018. <https://doi.org/10.1016/j.jafrearsci.2017.12.007> .
- [21] R. Leborgane, M. O. Rivett, G. J. Wanangwa, P. Sentenac. R. M. Kalin, "True 2-D Resistivity Imaging from Vertical Electrical Soundings to Support More Sustainable Rural Water Supply Borehole Siting in Malawi". *Appl. Sci.* vol. 11, no. 3. Jan, 2021. <https://doi.org/10.3390/app11031162> .
- [22] J. S. Whiteley ,J. E. Chambers,S. Uhlemann,P. B. Wilkinson,J. M. Kendall, "Geophysical Monitoring of Moisture-Induced Landslides: A Review". *Rev. Of Geophy.* vol. 57, no. 1, pp 106-145. Mar, 2019. <https://doi.org/10.1029/2018RG000603> .
- [23] *Geophysics for the Mineral Exploration Geoscientist*, M. Dentith, and S. Mudge, eds., New York, USA, NY : Univ. Cambridge Press, 2014. [Online]. Available <https://www.cambridge.org/de/academic/subjects/earth> .
- [24] *Applied Geophysics*, W.M. Telford L. P, Geldart, R.E Sheriff, eds., New York, USA, NY : Univ. Cambridge Press, 1990, <https://doi.org/10.1016/j.conbuildmat.2020.120765> .